Aggregate structures of the sorbitan monooleate (SPAN80) surfactant at TiO_2(rutile)/water interfaces by computer simulations

E. Núñez-Rojas and H. Domínguez
Instituto de Investigaciones en Materiales, Universidad Nacional Autónoma de México, México, D.F. 04510, México,
e-mail: eeddgar@yahoo.com.mx; hectordc@servidor.unam.mx

Received 21 March 2013; accepted 26 July 2013

Molecular dynamics simulations were carried out to study the behavior of a nonionic surfactant close to TiO_2 surfaces at three different crystallographic orientations of rutile, (001), (100) and (110). Sorbitan Monooleate (SPAN80) molecule was used as nonionic surfactant and it was observed that these molecules seemed to aggregate in similar ways. Namely, the hydrocarbon chains of the surfactant molecules were attached at the solid surfaces. Structure of the molecules and surfactant adsorption on the surfaces were studied in terms of tails and head groups density profiles as well as surface coverage. From density profiles and angular distributions it was possible to determine the influence of the solid surface. For instance, on the three surfaces the surfactant molecules formed molecular layers parallel to the surface. Besides, it was found that in the solids (100) and (110), where there were oxygen atoms exposed on the surface, surfactants were attached to the surfaces along the sites between the lines of these oxygen atoms. Finally, diffusion coefficients for the aggregates were calculated in order to determine molecular mobility on the surfaces. These results were compared with those of the Sodium Dodecylsulfate (SDS) molecules on the same rutile surfaces and it was found that the SPAN80 molecules were more attached to surfaces than the SDS molecules. On the other hand the diffusion coefficients calculated in the present work were also compared with those obtained in a SDS/graphite system and we observed that SDS molecules on graphite showed a significant mobility compared with the same molecules on rutile.

Keywords: Computer simulations; SPAN80 surfactant; adsorption; rutile.

Se realizaron simulaciones de dinámica molecular para estudiar el comportamiento de un surfactante no-iónico sobre una superficie de TiO_2 en las tres diferentes caras en la estructura de rutilo, (001), (100) y (110). Como surfactante se uso la molécula Sorbitan Monooleate (SPAN80) y se observó que las moléculas se adsorben sobre las diferentes superficies de manera similar. Para cada una de las superficies se vio que los surfactantes se agregaron con las colas hidrocarbonadas adsorbidas sobre las placas de rutilo. Se realizaron estudios de los perfiles de densidad y distribuciones angulares para estudiar la adsorción y se observó que las moléculas de surfactante se depositaron en capas paralelas sobre la superficie. En particular, se encontró que para las caras (100) y (110) los surfactantes se adsorbieron en el sólido entre los espacios de los átomos de oxígeno expuestos sobre las superficies . También se realizaron estudios del coeficiente de difusión para calcular la mobilidad del agregado formado sobre las superficies. Estos resultados se compararon con estudios previos del surfactante sulfato dodecil de sódio (SDS) sobre las mismas superficies y se encontró que las moléculas de SPAN80 se anclaban más sobre las superficies que el SDS. Sin embargo, cuando se compararon estos resultados, del coeficiente de difusión, de moléculas de SDS sobre una superficie de grafito se encontró que en este caso el SDS tenía una mobilidad mucho mayor en esta superficie que en las superficies de rutilo.

Descriptores: Simulaciones por computadora; surfactante SPAN80; adsorción; rutilo.

PACS: 68.08De; 68.43.Hn; 68.43.Jk

1. Introduction

The adsorption of surfactant molecules at solid surfaces has been studied for a long time due to its importance in industrial processes such as corrosion inhibition, dispersion stabilization, detergency, crude oil refining, treatment of waste water, adsorption on activated charcoal and even in pharmaceutical preparations where surfactant molecules are used to stabilize solid ingredients dispersed in water [1–3].

Self-assembled structures of nonionic surfactants at hydrophobic-solid/water interfaces have been investigated by several people and they have found, for instance, that adsorption isotherms exhibit strong interactions of surfactant molecules with the solid surface and level off well below the critic micellar concentration (CMC) which is the concentration of saturation at the interface. On the other hand curved aggregates have been generally observed ranging from monolayers to hemicylinders where a strong influence on the colloidal stability by the substrate has been noticed [4–6]

Adsorption and structures of molecules on surfaces have been studied by different experimental techniques such as streaming potential methods [7], calorimetry [8], neutron reflection [9], ellipsometry [10], fluorescence spectroscopy [11] and atomic force microscopy (AFM) [12]. In fact, by AFM it has been obtained detailed information about the topology of aggregation of surfactants, *e.g.* Manne et al. observed the self-assembling of Cetyltrimethylammonium Bromide (CTAB) molecules on a surface of graphite in parallel stripes [13] and similar morphologies have been seen for other surfactants on hydrophobic surfaces [6, 14, 15].

For such studies, different solid surfaces have been used as substrates such as graphite, gold, mica and titanium dioxide(TiO_2). In fact, among various semiconductor materials, TiO_2 has attracted much interest due to its potential

use in industry [16, 17]. It is a stable solid which is not soluble in water, it is not toxic and due to its high refraction index is by far the most white solid material known. For these reasons this material is used in the manufacture of many products of human consumption such as food, plastics, cleaners and coatings. Besides, it is also the main raw material in the production of white painting.

Surfaces of rutile have been subject of studies from both experimental and theoretical points of view [18, 19]. The adsorption and interaction of different surfactant molecules with TiO_2 have been also investigated [20–23]. Three different orientations, (001), (100) and (110) have been investigated experimentally [24] and by conducting studies of contact angles of water drops on these surfaces different hydrophobicities have been found; the surfaces (110) and (001) were the most hydrophobic ones, whereas the surface (100) showed a smaller hydrophobicity than that of graphite.

From the theoretical point of view some models have been proposed to describe nonionic surfactant adsorption, for instance, by considering an homogeneous adsorbed layer [25, 26] or by considering adsorption process in different stages [27]. The disadvantage of these models is that those assumptions are made on the segment density distributions in the adsorbed layer. Such assumptions, however, have not been required in modern statistical thermodynamic treatments, like the self-consistent-field theory [28].

From a computational perspective several studies have been conducted to study molecular aggregation at interfaces, for instance, Coarse-grained Monte Carlo investigations have provided useful information about morphological transitions of surfactant surface aggregation [29] while molecular dynamics simulations have been carried out to investigate aggregate properties at atomistic scales [30, 31]. Monolayers and their dynamics on a graphite surface have been also studied and it was found that graphite surfaces impose an orientational bias the carbon atoms in the solid due to the surfactant-solid interactions [31].

In a previous work we investigated structures of Sodium Dodecylsulfate (SDS) molecules on rutile surfaces [32]. Now, in the present paper we are interested in extending the studies using Sorbitan Monooleate (SPAN80), a nonionic surfactant molecule, on the same surfaces of rutile. We focus on how the different crystallographic orientations of the solid modify the surfactant structure on the surfaces and the mobility of the molecular aggregates on the same surfaces by calculating diffusive coefficients as a parameter to determine the level of molecular attachment on the solid.

2. Computational method and model

For the present study molecular dynamics simulations of surfactant molecules at three different rutile surfaces were carried out. The solids walls were constructed using an atomistic model for the surfaces (110), (100) and (001) [32].

For the surfactant molecule we used a Sorbitan Monooleate (SPAN80) model of 17 united carbon atoms attached to a head group, where the head group atoms were explicitly modeled (see Fig. 1). The initial configuration was prepared from a monolayer of 25 surfactant molecules in all-trans configuration with the SPAN80 head groups initially pointed to the solid surface and placed close to the rutile surface. Then 2535 water molecules were added (using the SPC model [33]) to the system.

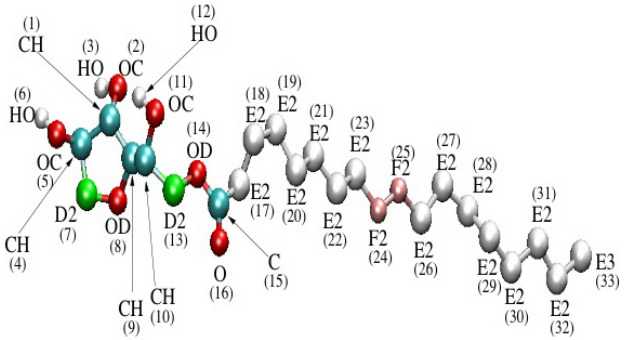

FIGURE 1. Bond potential parameters for atoms of the SPAN80 molecule showed in Fig. 1 (Eq. 2).

TABLE I. Bond potential parameters for atoms of the SPAN80 molecule showed in Fig. 1 (Eq. 2).

Bond	k_r(kcal/(mol Å^2))	r_{eq}(Å)
CH - OC	772	1.43
HO - OC	1106	0.96
CH - CH	520	1.53
F2 - F2	1140	1.31
F2 - E2	520	1.53
CH - D2	520	1.53
D2 - OD	640	1.43
OD - C	980	1.34
O - C	1140	1.23
C - E2	634	1.52
E2 - E2	620	1.53
E2 - E3	620	1.53

The number of molecules corresponded to a high concentration used in real experiments (≈0.43 M) [34], therefore with this number we guaranteed that aggregation was observed in the present simulations.

The usual periodic boundary conditions in the X and Y directions were imposed in the simulations, however, the Z-dimension the box was set to 150 Å. This length was long enough to prevent the formation of a second water/solid interface due to the periodicity of the system. Instead, a liquid/vapor interface was present at one end of the box (Z>0).

All simulations were carried out in the NVT ensemble with a time step of 0.002 ps using DL-POLY package [35]. Bond lengths were constrained using SHAKE algorithm with

TABLE II. Valence angle potential and dihedral angle potential parameters for atoms of the SPAN80 molecule showed in Fig. 1 (Eqs. 3, 4 (R-B potential) and 5 (cosine potential form)).

Sorbitan Monooleate		
group	K_{ang}, (kcal/mol rad^2) θ_0 (rad)	torsion, A (kcal/mol), δ (rad), m
CH - OC - HO	110, 108.5	
CH - CH - OC	160, 109.5	
CH - CH - D2	126, 115.5	
CH - CH - OD	160, 109.5	
CH - CH - CH	126, 115.5	
CH - D2 - OD	160, 109.5	
D2 - OD - CH	200, 109.5	
D2 - OD - C	200, 109.5	
OD - C - O	180, 126.0	
OD - C - E2	110, 109.0	
C - E2 - E2	126, 112.4	
O - C - E2	140, 125.4	
E2 - F2 - F2	126, 115.4	
E2 - E2 - E2	126, 112.4	
E2 - E2 - E3	126, 112.4	
E2 - E2 - E2 - E3		R-B[a]
E2 - E2 - E2 - E2		R-B[a]
CH - CH - D2 - OD		14.000, 180.00,cos
CH - CH - OC - HO		0.5000, 0.0000,cos
CH - CH - OC - OH		14.000, 180.00,cos
CH - CH - OD - D2		1.0000, 180.00,cos
CH - CH - CH - OC		2.0000, 0.0000,cos
CH - CH - CH - D2		2.0000, 0.0000,cos
OC - CH - CH - OC		14.000, 180.00,cos
OC - CH - CH - D2		14.000, 180.00,cos
OC - CH - CH - OD		14.000, 180.00,cos
OH - OC - CH - CH		14.000, 180.00,cos
CH - D2 - OD - C		1.4500, 0.0000,cos
D2 - OD - C - O		5.5600, 180.00,cos
D2 - OD - C - E2		1.0000, 180.00,cos
OD - C - E2 - E2		0.0000, 180.00,cos
O - C - E2 - E2		0.0000, 180.00,cos
E2 - E2 - F2 - F2		2.0000, 0.0000,cos
E2 - F2 - F2 - E2		2.0000, 0.0000,cos
F2 - F2 - E2 - E2		2.0000, 0.0000,cos

a) R-B (kcal/mol) c'_0=1.9872, c'_1=0.0000, c'_2=3.0000, c'_3=0.5000, $c'_4 = 0.0000$

TABLE III. Lennard-Jones parameters of each atom of the SPAN80 molecule.

Atom	ϵ (kcal/mol)	σ (Å)
CH - CH	0.0800	3.8505
OC - OC	0.1500	3.1000
HO - HO	0.0000	0.0000
D2 - D2	0.1180	3.9057
OD - OD	0.1700	2.9934
C - C	0.1050	3.7507
OS - OS	0.2100	2.9578
E2 - E2	0.1180	3.9050
F2 - F2	0.0800	3.8505
E3 - E3	0.1750	3.905

TABLE IV. Electrostatic charge of each atom in the SPAN80 molecule (Fig. 1).

Atom of the SPAN80 molecule	q (e)
1	0.1286
2	-0.2900
3	0.1856
4	0.1071
5	-0.2811
6	0.1801
7	0.1171
8	-0.2421
9	0.1101
10	0.1501
11	-0.2801
12	0.1776
13	0.1401
14	-0.2511
15	0.3121
16	-0.2641
17 - 33	0.0000

a tolerance of 10^{-4} and the temperature was controlled using the Hoover-Nose thermostat with a relaxation time of 0.2 ps [36] at T=298 K. The long-range electrostatic interactions were handled with the Particle Mesh Ewald method, and the Van der Waals interactions were cut off at 10 Å. Finally, all simulations were run up to 40 ns and configurational energy was monitored as a function of time to determine when systems reached equilibrium. Then, we collected data from the last 2 ns for analysis.

The simulation parameters for the solid surface and the water molecules were taken from previous works [32, 37], and the parameters for the SPAN80 molecule are summarized in Tables I - IV [38]. In the case of the surfactant molecule

it was not possible to find parameters in the literature, therefore they were determined as a combination of first principle quantum calculations and data from an already reported force field [39]. The parameters used in the simulations are indicated in Tables I - IV.

The total intramolecular potential for the surfactant included bond, angular and torsional potentials,

$$E = E_{\text{bond}} + E_{\text{ang}} + E_{\text{tor}} \quad (1)$$

The bond lengths were modeled by an harmonic potential,

$$E_{\text{bond}} = K_b(r - r_0)^2 \quad (2)$$

where r_0 is the equilibrium distance between two bonded atoms and K_b is the bond constant (Table I). The angles in the chain were also constrained by an harmonic potential,

$$E_{\text{ang}} = K_\theta(\theta - \theta_0)^2 \quad (3)$$

where θ_0 is the equilibrium angle and K_θ is the force constant (Table II). The torsional angles were modeled by the Ryckeart and Bellemans (R-B) potential [40] for the tails whereas a cosine potential form was used for the head group,

$$E_{\text{tor-RB}} = \sum_{k=0}^{5} c_k \cos^k(\phi) \quad (4)$$

$$E_{\text{tor-cos}} = A[1 + \cos(m\phi - \delta)] \quad (5)$$

where the c_k are the energy constants and ϕ is the dihedral angle. The potential parameters are given in Table II.

3. Results

In this section we present the calculations performed on the SPAN80 surfactant on the three different rutile surfaces. Studies on the behavior of the SPAN80 molecules and how they aggregated at the liquid/solid interfaces are discussed. Besides, the mobilities of the molecular aggregates were determined by calculating diffusion coefficients and we carried out simulations for Sodium Dodecylsulfate (SDS) molecules on the same rutile surfaces to compare the results.

3.1. Density profiles

In order to see where the surfactant molecules arrayed in the system the mass Z-density profiles for the head groups and the tails were calculated, *i.e.* normal to the liquid/solid interface.

Figure 2a shows the density profiles calculated along the Z-direction for the surfactant molecules interacting with the solid surface (001). From the figure we observed a layer of SPAN80 molecules on the surface attached by their hydrophobic tails and their head groups (first peak of the solid line and first peak of the dashed line in the density profiles).

Moreover, it was also possible to depict the formation of a second and a third layer of both tail groups and head groups.

Figure 2b shows the density profiles of SPAN80 molecules on the solid surface (100). Although a similar behavior was observed of that on the surface (001) in this case the profiles shown strong peaks suggesting that the SPAN80 molecules arrayed in well defined layers parallel to the surface. In the same figure it was possible to observe that the molecules were better packed than the molecules on the surface (001) since the density profiles for the head groups and the tail groups ended at $Z\approx$-8 Å, while the density profiles in the case of the surface (001) ended at $Z\approx$-5 Å.

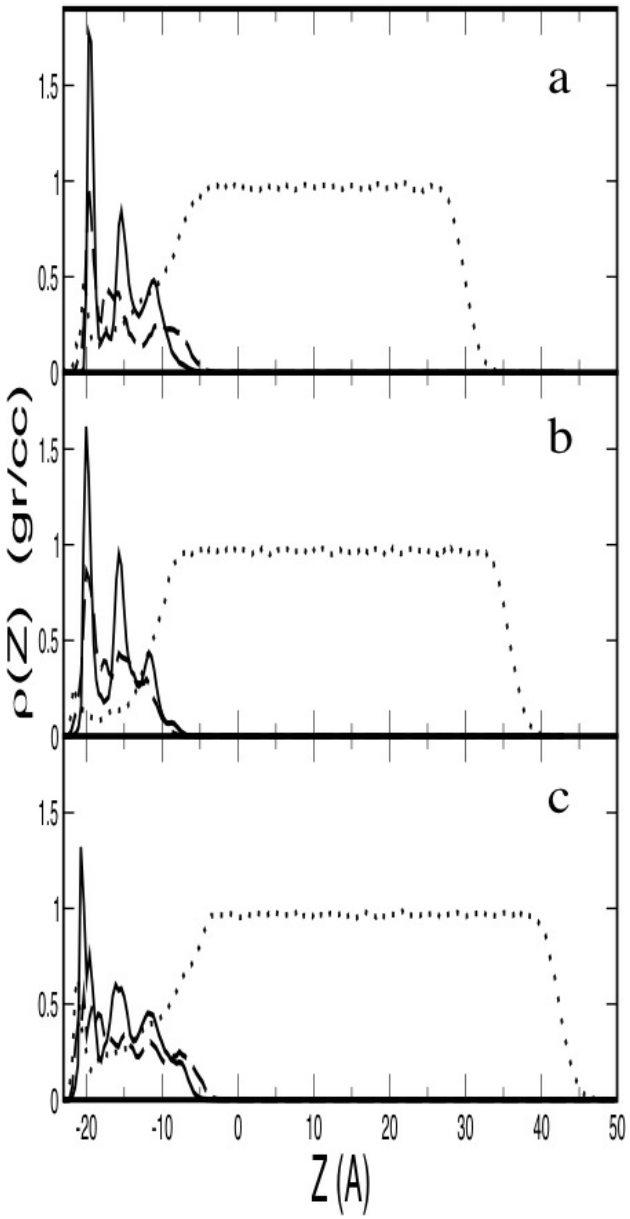

FIGURE 2. SPAN80 Z-density profiles for molecules on the rutile solid surfaces. The dotted line represents water, the dashed line the head groups and the solid line the tail groups of the surfactant molecules. The solid surface is located at the left of the plot. a) (001), b) (100) and c) (110).

The density profiles of the SPAN80 molecules on the surface (110) are shown in Fig. 2c. In this figure a similar behavior to that observed in the solid surfaces (001) was also depicted, *i.e.* the surfactant molecules were attached to the surface by the tail groups. These results suggested that even though solid surfaces have different atomistic configuration the surfactant molecules underwent a similar attraction. Besides, the head group density profile was not as well defined as the tail group density profile. These results suggested that for the three solid surfaces the hydrophobic behavior prevails.

When the present results were compared with those obtained for Sodium Dodecylsulfate (SDS) molecules on the same surfaces [32] a different behavior was observed. For instance on surface (110) the SDS molecules were attached only by their polar groups while SPAN80 molecules were clearly attached by the hydrophobic chains and the polar groups.

3.2. Coverage and adsorbed layer

Since surfactant molecules might cover surfaces in different ways depending on the properties of the solid surfaces and of the solid-surfactant interactions an important parameter to study adsorption usually is the coverage. In the present work we measured coverage as the relation between the area occupied by the SPAN80 molecules aggregated with the total area of the surface. Moreover, in order to determine if there were any preferred adsorption sites in the solid surfaces we also studied the first adsorbed layer in all the systems. The first adsorbed layer was defined by the first peak in the density profiles.

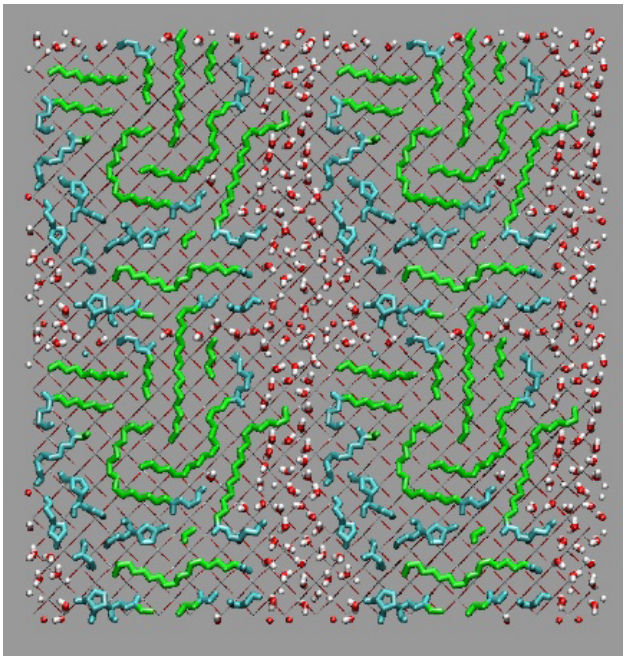

FIGURE 3. Snapshot (XY plane) of the final configuration of the adsorbed molecules on the (001) surface. The green structures correspond to hydrocarbon chains, the blue structures correspond to head groups and the water molecules are represented by structure white and red.

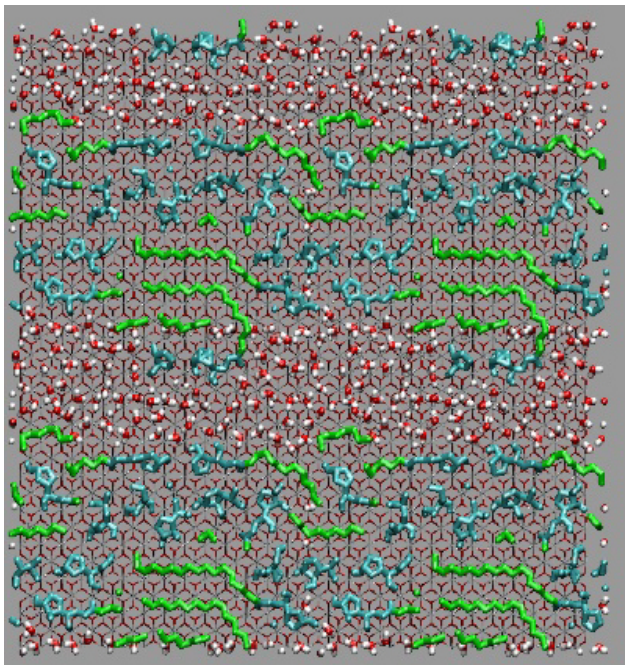

FIGURE 4. Snapshot (XY plane) of the final configuration of the adsorbed molecules on the (100) surface. The colors represent the same as in Fig. 3.

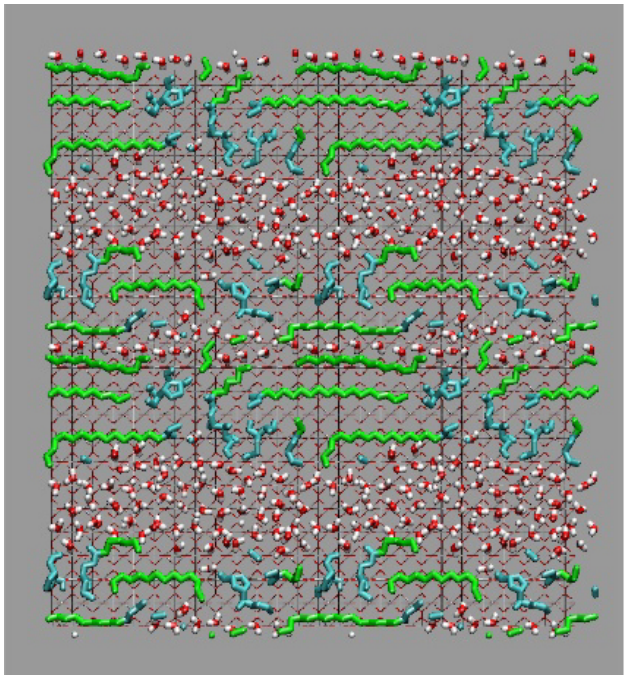

FIGURE 5. Snapshot (XY plane) of the final configuration of the adsorbed molecules on the (110) surface. The colors represent the same as in Fig. 3.

In Figs. 3, 4 and 5 the representative snapshots of the first adsorbed layers of all the systems are shown. In order to improve visualization these surfaces were duplicated in both X-axis and Y-axis. Moreover, in the figures some molecules

look like incomplete since the figures show only atoms in the adsorbed layer.

Figure 3 shows the final configuration of the first adsorbed layer on the surface (001). In this case we observed that SPAN80 molecules covered ≈ 85 % of the solid surface. Also, in Fig. 4 a representative configuration of the first adsorbed layer on the surface (100) is shown. In this case the coverage was ≈ 91 % and it was possible to observe that surfactant molecules seemed to aggregate in an ordered structure.

Finally, for this study in Fig. 5 the final configuration of the first adsorbed layer on the surface (110) is also shown, where it was obtained a coverage of ≈ 83 % and we observed from that picture that the surfactant molecules were also adsorbed in an oriented way.

It was also possible to locate the sites on the rutile surfaces where the SPAN80 molecules (of the first adsorbed layer) were adsorbed; it was made by analyzing the tails and head groups density profiles along the Y axis with those of the oxygen superficial atoms of the TiO_2 surfaces. In Fig. 6a the profiles for the surface (100) are shown. The position of the oxygen atoms on the surface were depicted by the dashed lines and the SPAN80 molecules by the solid lines. We observed that the SPAN80 molecules were located between the oxygens, *i.e.* the profiles indicated that the molecules were adsorbed between the superficial oxygen atoms of the solid. For the surface (110), the surfactant molecules (solid lines in Fig. 6b) were also located between the gaps of the upper oxygens atoms on the surface. For the surface (001) we did not observe any particular orientation of the molecules attached on the surface. The results about a preferential site for adsorption are similar to those obtained in the simulations with SDS molecules [32].

On the other hand, adsorption of the molecules was also analyzed by studying potential energy surfaces. In this case it was evaluated the potential energy between the rutile plate

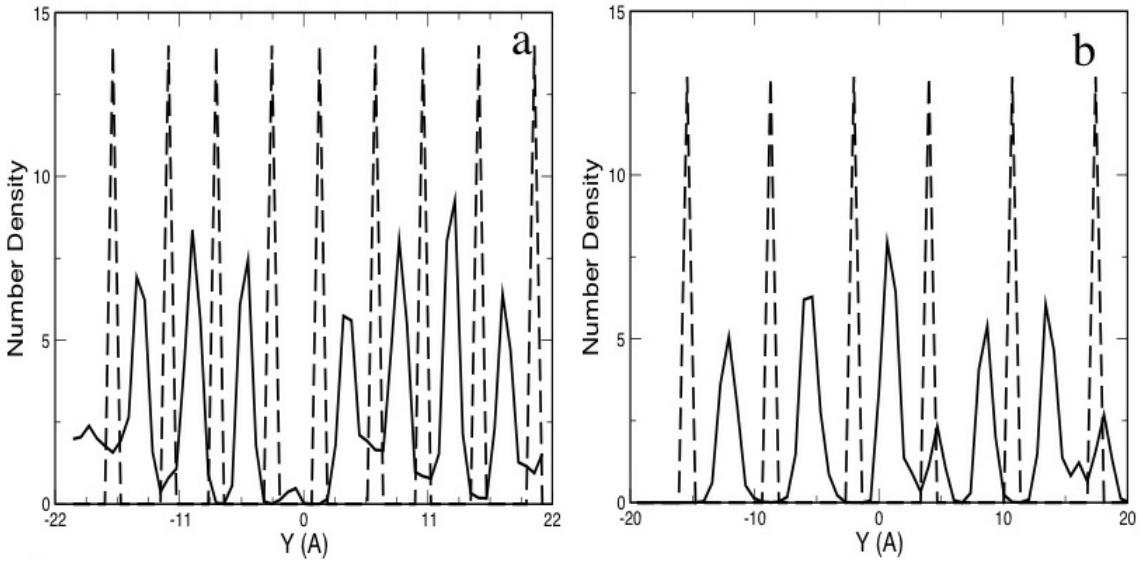

FIGURE 6. Number density profiles in the Y-axis. for the surfactant molecules in the first adsorbed layer. The dashed line corresponds to oxygen atoms in the surface and the solid line corresponds to the SPAN80 molecules. a) Surface (100) and b) Surface (110).

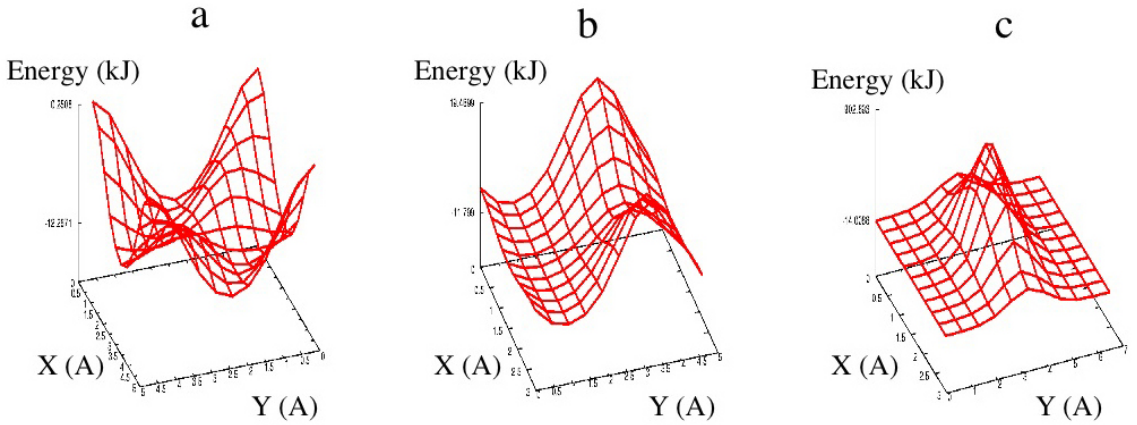

FIGURE 7. Potential Energy profiles of the unit crystal cells of rutile with SPAN80 hydrocarbon chains. a) (001), b) (100) and c) (110). Note the difference in the scale energy axis.

and the first adsorbed layer of the tails (calculated in the density profiles). Then, a energy profile in the Z-direction was calculated on the respective unit cells of each surface. Since the tails did not have electrostatic interactions with the rutile surfaces the energy profiles were given only in terms of the LJ potential.

The potential profiles on the three different unit crystal cells were calculated (in the Z position which corresponded to the first peak in the density profile) and they are shown in Fig. 7. It was found that the minimum energy for the surfaces (001), (100) and (110) were -12.27, -11.79 kJ and -14.01 kJ, respectively. Similar order of magnitude in the energy has been found in experiments for one CH_2 group involved in aggregation [41].

It is important to notice that on both surfaces (100) and (110) the maximum energies in the profiles were located on the superficial oxygen atoms of the rutile plates, *i.e*. there was some kind of energy barrier on those positions. Therefore, it was not observed surfactant molecules along those atoms. In fact, the results can explain why the surfactants arrayed with an ordered orientation on the surfaces (along the sites where the energy is minimum). On the other hand, in the surface (001) the difference between the maximum and the minimum energy values was small ($\Delta U \approx 12.5$ kJ) and it might be the reason why on this surface the surfactants did not array with any privileged orientation. All these results were in agreement with the density profiles in the 'Y' direction calculated previously.

3.3. Orientation and total length of hydrocarbon chains

Information of how the molecules were arrayed at the different surfaces was also obtained from the length of the hydrocarbon tails. Therefore, the length was measured as the distance from the last carbon to the first one closer to the head group with the following equation;

$$\langle \mathbf{R} \rangle = \frac{1}{P}\frac{1}{N}\sum_{i=1}^{N,P} \Delta \mathbf{r}_i \qquad (6)$$

N is the total number of SPAN80 molecules, P is the number of configurations in the last 2 ns of simulation and

$$\Delta \mathbf{r}_i = \sqrt{(\Delta X)_i^2 + (\Delta Y)_i^2 + (\Delta Z)_i^2} \qquad (7)$$

where ΔX is the distance from the last to the first carbon atoms in the hydrocarbon chain in the X coordinate. Similar definitions were given for ΔY and ΔZ. From these calculations we observed that larger tails were obtained on the surfaces (110) (l=17.35 Å) and (100) (l=16.89 Å) than on the surface (001) (l=16.14 Å), however all of them were smaller than the length chain in its all-trans configuration (l=20.3 Å).

We also calculated the orientation of the hydrocarbon chains with respect to the vector normal to the interface by measuring the angle θ by using the equation;

In Fig. 8a the angular distribution of the hydrocarbon chains with the surface (001) is shown where we observed a

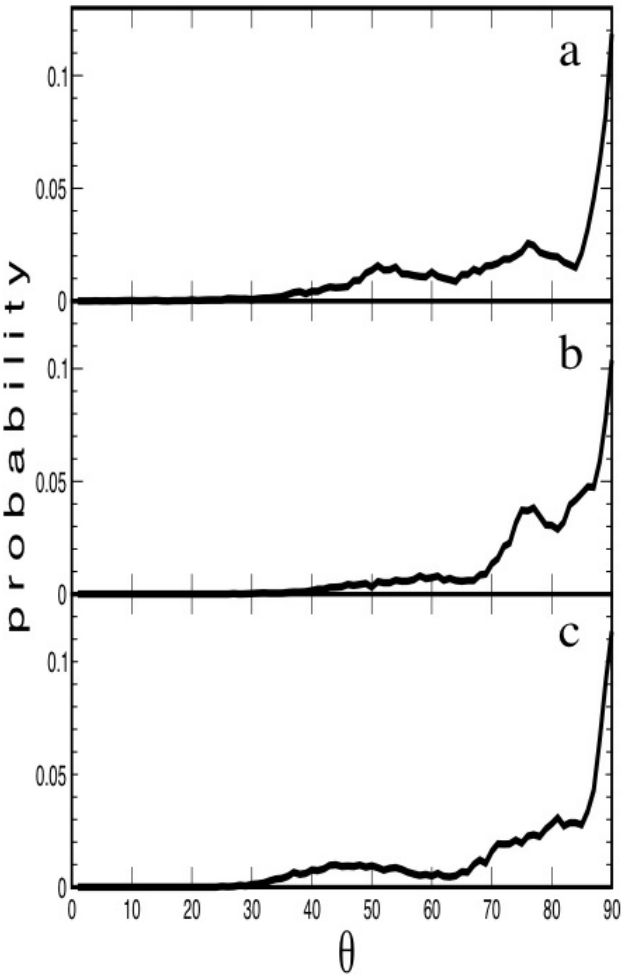

FIGURE 8. Angular distribution of hydrocarbon chains with respect to the vector normal to the interface on the solid surfaces. a) (001), b) (100), and c) (110).

tendency of the tail groups to be perpendicular to the vector normal to the surface, *i.e*., several hydrocarbon chains were parallel to the solid surface. However, it was also possible to observe two peaks around 50 degrees and around 78 degrees, which indicated that some molecules were not totally parallel to the solid surface.

In Fig. 8b we observed again that the tail groups showed the tendency to be parallel to the surface (100). In this case it is possible to observe a peak around 75 degrees which suggested that not all the hydrocarbon chains were totally parallel to the solid surface, although they were more oriented than the molecules on the (001) surface.

Finally in Fig. 8c the angular distribution of the tail groups of the molecules on the surface (110) is shown. Here the molecules showed again a tendency to be oriented perpendicular to the normal vector to solid surface.

3.4. Mobility of SPAN80 and SDS aggregates on the surfaces

From previous simulations, in our group, of SDS molecules on graphite surfaces we observed that aggregates were not

completely anchored to the surface, *i.e*, aggregates present some kind of mobility on the plate [42]. We characterized the mobility by calculating the diffusion coefficient of all the surfactants in the aggregate. In fact, by measuring mobility of the molecules we might know, somehow, information about the strength of the interaction between the adsorbed surfactant molecules and the solid surfaces.

The diffusion coefficient was calculated by the square mean displacements in all direction. The coefficient along X direction was defined as,

$$2D_{xx} = \frac{\langle \Delta X^2(t) \rangle}{t} \tag{8}$$

where

$$\langle \Delta X^2(t) \rangle = \langle [X(0) - X(t)]^2 \rangle \tag{9}$$

with similar expressions for Y and Z directions.

For the X, Y and Z directions we obtained values of 0.2783×10^{-9} m^2/s, 0.1164×10^{-9} m^2/s and 0.0172×10^{-9} m^2/s, respectively [42]. Since the aggregate was adsorbed on the surface (in XY plane) the smallest diffusion was obtained in the Z-direction, *i.e*. the aggregate remained on the plane. However, by direct observation of the aggregate on the surface, at different times, we noted some motion of it along the X direction. In that case the diffusion coefficient was the largest, *i.e.* one order of magnitude of that in the Z-direction.

For the present study we also investigated if the SPAN80 aggregates present some mobility on the rutile surfaces. Moreover, since in our previous work [32] we report structural studies of SDS aggregates on the same rutile surfaces, in this paper we also did the same study of mobility to compare the results with those of the SPAN80.

In Table V the diffusion coefficients for the SDS aggregates on the three different solid surfaces of rutile are shown. It is observed that the smallest coefficient was obtained on the surface (100). The result suggested that the molecular aggregate on this surface was more tied to the solid than in the other surfaces. In fact, from a previous work [32] it was possible to observe that molecules aggregated and packed themselves on this surface in the most ordered way.

In contrast with the results on the graphite surface it was not observed any mobility of the aggregates on any of the rutile surfaces (by looking at the aggregate at different simulation times from a movie of the configurations).

Also in the Table V the diffusion coefficients for the SPAN80 molecules on the rutile surfaces are shown where it can be observed that all the coefficients are smaller than the coefficients calculated for the SDS molecules. However, the difference can be understood by taking into account that the SPAN80 molecule has a larger hydrocarbon chain than the SDS molecule, therefore, a stronger hydrophobic effect is present in SPAN80. As well as in the case of the SDS aggregate it was not observed any kind of mobility on the surface (from the configurations).

TABLE V. Diffusion coefficients calculated in the three different directions of the rutile surfaces for the SDS aggregate, SPAN80 aggregate and the adsorbed layers of both surfactant molecules.

SDS Aggregate			
Rutile	(001)	(100)	(110)
D_{xx} (10^{-9} m^2/s)	0.06532	0.03297	0.09095
D_{yy} (10^{-9} m^2/s)	0.11405	0.03588	0.07253
D_{zz} (10^{-9} m^2/s)	0.04142	0.01099	0.06608
SPAN80 Aggregate			
D_{xx}	0.023803	0.023909	0.016482
D_{yy}	0.023724	0.020266	0.021058
D_{zz}	0.010611	0.010306	0.009397
SDS adsorbed layer			
D_{xx}	0.00898	0.00355	0.00810
D_{yy}	0.00461	0.00281	0.00274
D_{zz}	0.00326	0.00157	0.00121
SPAN80 adsorbed layer			
D_{xx}	0.00711	0.00674	0.00175
D_{yy}	0.00469	0.00322	0.00125
D_{zz}	0.00220	0.00208	0.00069

All previous results were given for the diffusion coefficient of all molecules in the aggregate, however, we also did calculations of the diffusion of the SDS molecules over the first adsorbed layer on the surface (Table V). As it was expected these values were smaller than those of the whole aggregate since molecules on the first layer were completely adsorbed on the surface, *i.e.* the molecules were totally attached to the wall.

Similar tendency was observed for the SPAN80 surfactant on the rutile surfaces (Table V) *i.e*. the coefficients had the same order than those calculated for the SDS molecules.

It is important to mention that in all cases the diffusion coefficient was smaller in the 'Y' direction than in the 'X' direction. For the surfaces (100) and (110) this result came from the structural differences of the solid surfaces since molecules were adsorbed along the 'X' direction where the lines of oxygen atoms in the wall were located.

4. Conclusions and discussion

We performed a series of molecular dynamics simulations of Sorbitan Monooleate SPAN80 nonionic surfactant molecules at three different rutile/water interfaces. Solid surfaces were built using different orientations of a crystalline cell, namely (001), (100) and (110) orientations.

We studied the structure of surfactant molecules on the rutile surfaces and from the density profiles some similarities on the different surfaces were depicted. Basically the surfactant molecules were attached by the hydrocarbon chains and the head group on all surfaces. In fact, those plots calculated

in the three surfaces showed a structure of layers formed by hydrocarbon chains parallel to the surface indicated by the peaks in the profiles. This behavior suggested the hydrophobicity of the rutile surface as it has been observed experimentally [24].

The sites where the SPAN80 molecules were adsorbed in the solid surface were also analyzed and it was found that molecules of the first layer on the surface (100) were adsorbed by the tail groups and head groups. Moreover, they were located between the superficial oxygen atoms of the surface. Similar trends were depicted on the surface (110). However, for surface (001) we did not observe any tendency of the surfactants to be adsorbed in specific sites of the surface.

Surface coverage was also studied and it was observed that the solid surface (110) had the smallest coverage and the surface (100) the largest one. This result is a consequence of the density of adsorption sites in the surfaces.

The influence and affinity of the solids over the aggregates were also determined by the way the tails were structured on the surface, the length, the adsorption and the orientation of the molecules on the different walls. Then, the average total length of the tail groups was calculated and it was found that for surfactant molecules on the surface (110) the length chains reduced 14.5% of the full extended chain whereas in the surface (100) and (001) the reduction was 16.8% and 20.3%, respectively.

Comparisons of the present results with those of Sodium Dodecylsulfate (SDS) surfactant on the same rutile surfaces were conducted and, as experiments have shown, we concluded that when the hydrocarbon chain increased the hydrophobic effect also increased, *i.e*, attraction between hydrophobic surfaces and molecules with long hydrocarbon chains was high.

On the other hand we also observed that SDS and SPAN80 might array in different ways on the same surface, for instance in the surface (110) the SDS molecules were attached over the titanium atoms by their polar groups [32] whereas the SPAN80 molecules were attached by both the head and the tail groups. This result makes evident the importance of the electrostatic interactions in molecular adsorption.

Finally, mobility of the aggregates on the surfaces were investigated. From previous simulations we observed that SDS surfactants formed semicilyndrical-like shape on a graphite surface where the whole aggregate present some movements on the surface (*i.e.* it did not keep completely fixed). Therefore, we analyzed if SPAN80 aggregates also present some mobility on the surfaces and we compared those results with the SDS surfactants on the same rutile surfaces. The mobility was characterized by calculating the diffusion coefficients in all three directions. It was observed that both surfactants, SDS and SPAN80, did not move on any of the rutile surfaces. By comparing the values of the diffusion coefficients we noted that aggregates on rutile had diffusion one order of magnitude lower than that of the aggregates on graphite. Actually, from the present results, it seems that in order to observe any movement of the aggregates on the surfaces the diffusion coefficient should have a value above 0.2×10^{-9}, although it is necessary to conduct more simulations with more surfactants and different surfaces to make a general statement about this issue (we are currently carrying out some simulations on this direction).

5. Acknowledgments

We acknowledge support from grants DGAPA-UNAM-Mexico, IN102812 and Conacyt-Mexico,154899. We also thank DGTIC-UNAM for KamBalam supercomputer facilities. ENR acknowledges the scholarship and support from CONACyT Mexico.

1. M. Ahmaruzzaman and D. K. Sharma, *J. Colloid Interf. Sci.* **287** (2005) 14.
2. A. Bhatnagar and A. K. Jain, *J. Colloid Interf. Sci.* **281** (2005) 49.
3. I. F. Uchegbu and A. G. Schtzlein, *Polymers in Drug Delivery*, (CRC Press. Taylor and Francis Group, LLC., 2006).
4. D. Furlong and J. R. Aston, *Coll. Interf.*, **4** (1982) 212.
5. L. Grant and W. J. Ducker, *Phys. Chem. B*, **101** (1997) 5337.
6. H. N. Patrick, G. G. Warr, S. Manne, and I. A. Aksay, *Langmuir* **13** (1997) 4349.
7. D. W. Fuerstenau, *J. Phys. Chem.* **60** (1956) 981.
8. Z. Király and G. H. Findenegg, *J. Phys. Chem. B* **102** (1998) 1203.
9. J. Penfold, E. J. Staples, I. Tucker, and L. J. Thompson, *Langmuir* **13** (1997) 6638.
10. F. Tiberg, B. Joensson, and B. Lindman, *Langmuir* **10** (1994) 3714.
11. P. Chandara, P. Somasundaranan, and N. J. Turro, *J. Colloid Interf. Sci.* **117** (1987) 31.
12. W. A. Ducker and E. J. Wanless, *Langmuir* **12** (1996) 5915.
13. S. Manne, J. P. Cleveland, H. E. Gaub, G. D. Stucky, and P. K. Hansma, *Langmuir* **10** (1994) 4409.
14. M. Jaschke, H. J. Butt, H. E. Gaub, and S. Manne, *Langmuir* **13** (1997) 1381.
15. W. A. Ducker and E. J. Wanless, *J. Phys. Chem. B* **100** (1996) 3207.
16. A. Heller, A*cc. Chem. Res.* **28** (1995) 503.
17. M. R. Hoffmann, S. T. Martin, W. Choi, and D. W. Bahnemann, *Chem. Rev.* **95** (1995) 69.

18. M. Ramamoorthy and D. Vanderbilt, *Physical Review B* **49** (1994) 16721.
19. S. Horikoshi, D. Minami, Seya Ito, H. Sakai, D. Kitamoto, M. Abe, and N. Serpone, *J. Photochemistry and Photobioloy A: Chemistry* **217** (2011) 141.
20. K. Esumi, K. Sakai, K. Torigoe, T. Suhara, and H. Fukui, *Colloids and Surfaces A: Physicochemical and Engineering Aspects* **155** (1999) 413.
21. S. Fukushima and S. Kumagai, *J. Colloid Interf. Sci.* **42** (1973) 539.
22. K. Esumi, A. Toyoda, M. Goino, T. Suhara, H. Fukui, and Y. Koide, *J. Colloid Interf. Sci.* **202** (1998) 377.
23. N. H. Tkachenko, Z. M. Yaremko, C. Bellman, and M. M. Soltys, *J. Colloid Interf. Sci.* **299** (2006) 686.
24. R. Wang, N. Sakai, A. Fujishima, T. Watanabe, and K. Hashimoto, *J. Phys. Chem. B* **103** (1999) 2188.
25. L. K. Koopal, G. T. Wilkinson, and J. Ralston, *J. Colloid Interf. Sci.* **126** (1988) 493.
26. J. F. Scamehorn, R. S. Schechter, and W. H. Wade, *J. Colloid Interf. Sci.* **85** (1982) 463.
27. N. A. Klimenko, V. Y. Polyakov, and A. Permilovskaya, *Kolloidn Zh. Sci.* **36** (1979) 861.
28. M. R. Bhömer and L. K. Koopal, *Langmuir* **6** (1990) 1478.
29. F. Zheng, X. Zhang, W. Wang, and W. Dong, *Langmuir* **22** (2006) 11214.
30. K. Shah, P. Chiu, M. Jain, J. Fortes, and B. Moudgil, S. Sinnott, *Langmuir* **21** (2005) 5337.
31. H. Dominguez, *J. Phys. Chem. B* **111** (2007) 4054.
32. E. Núñez-Rojas and H. Domínguez, *J. Colloid Interf. Sci.* **364** (2011) 417.
33. H. J. C. Berendsen, J. R. Grigera, and T. P. Straatsma, *J. Phys. Chem. B* **91** (1992) 6269.
34. J. Santhanalakshmi and S. I. Maya, *Proc. Indian Acad. Sci. (Chem. Sci.)* **108** (1997) 27.
35. T. R. Forester and W. Smith, *DL-POLY Package of Molecular Simulation*, (CCLRC, Daresbury Laboratory: Daresbury, Warrington, England, 1996).
36. W. G. Hoover, *Physical Review A* **31** (1985) 1695.
37. H. Dominguez, A. Gama Goicoechea, N. Mendoza, and J. Alejandre, *J. Colloid Interf. Sci.* **297** (2006) 370.
38. D. I. Salgado-Blanco, *MSc Thesis*, (Instituto de Investigaciones en Materiales,Universidad Nacional Atónoma de México, 2010).
39. S. J. Weiner *et al*., *J. Am. Chem. Soc.*, **106** (1984) 765.
40. J.P. Ryckeart and A. Bellemans, *Chem. Phys. Lett.* **123** (1975) 30.
41. J. Leimbach, *Colloid Surfaces A. Physicochem. Eng. Aspects* **94** (1995) 1.
42. E. Nuñez- Rojas, *PhD. Thesis, May, Instituto de Investigaciones en Materiales*, (Universidad Nacional Atónoma de México 2012).